EurJOC European Journal of Organic Chemistry

FULL PAPER

DOI: 10.1002/ejoc.201402178

The Side Chain Makes the Difference: Investigation of the 2D Self-Assembly of 1,3,5-Tris[4-(4-pyridinyl)phenyl]benzene Derivatives by Scanning Tunneling Microscopy

Daniel Trawny,[a] Lucie Vandromme,[a] Jürgen P. Rabe,*[b] and Hans-Ulrich Reissig*[a]

Keywords: C–C coupling / Monolayers / Star-shaped compounds / Self-assembly / Scanning probe microscopy

Flexible and straightforward syntheses of a series of D_{3h}- or C_{3h}-symmetrical star-shaped compounds with pyridine end groups are reported. In all cases, the acid-mediated cyclocondensations of the corresponding aryl methyl ketone provided the central benzene ring. For the preceding preparation of the functionalized compound arms, Suzuki couplings were applied. The crucial introduction of the pyridine C-2 and C-6 substituents occurred by Fe(acac)$_3$-catalyzed alkylations (acac = acetylacetonate). The preparation of the C_3-symmetrical compound involved an alternating sequence of halogenations and coupling reactions. The self-assembly behavior of the four resulting star-shaped compounds at the interface between 1-phenyloctane and the basal plane of highly oriented pyrolytic graphite (HOPG) was studied by scanning tunnelling microscopy (STM). We found self-assembled monolayers with structures strongly dependent on the substitution patterns of the investigated compounds. The reduction of the symmetry from a D_{3h}- to a C_{3h}-symmetrical compound led to an entirely different self-assembly behavior with the change from a hexagonal to a lamellar arrangement.

Introduction

The self-assembly of molecules into well-defined supramolecular architectures is a fundamental principle in nature and can be found in many biological and chemical processes.[1] Over the last decade, it became possible to construct molecular architectures with nanometer precision for technological applications, for example, in organic electronics[2] and molecular machines.[3] Supramolecular architectures at solid–liquid interfaces have been widely studied by scanning tunneling microscopy (STM), which is a powerful tool for investigation of the self-assembly of two-dimensional adsorbates.[4] The application of computational molecular dynamic methods makes it possible to predict self-assembly with increasing accuracy, but it is still a demanding task to anticipate and to control the 2D arrangement of molecular components.[5] Precise and systematic investigations of molecule-to-molecule interactions with STM could lead to an improved understanding of the complex self-assembly processes.

The investigation of the self-assembly of C_3-symmetrical ("star-shaped") compounds with pyridine end groups at the solution–graphite interface is particularly interesting as the molecular C_3 scaffold fits perfectly to the graphite lattice. In previous studies, we reported a new C_3-symmetrical tris(oxazole) derivative and its ability to form self-assembled monolayers.[6] Although we expected the formation of a hexagonal arrangement, the C_{3h}-symmetrical trisoxazole derivative self-assembled into long chains, and a lamellar lattice was observed. A literature analysis showed that the self-assembly of D_{3h}- and C_{3h}-symmetrical molecules has rarely been investigated.[7] To clarify the influence of the substitution pattern of star-shaped compounds, we planned to prepare a series of model compounds with D_{3h} or C_{3h} symmetry and to investigate their self-assembly by STM. The different pyridyl end groups offer additional options for further experiments at interfaces.

The preparation of this type of compound can be envisioned by three synthetic strategies, as depicted in Scheme 1. The star-shaped pyridine derivatives consist of three parts: ligands, spacers, and a core unit. Pathways A and B (Scheme 1) exemplify two common approaches that use coupling reactions such as Sonogashira or Suzuki reactions to connect the core, spacer, and ligand moieties. The spacer moiety may be either at the core unit (pathway A) or at the ligand (pathway B).[8] The third strategy, is illustrated by pathway C (Scheme 1), which involves a trimerization process to construct the central core from three functional ligand–spacer units. One option to achieve this goal is the cyclocondensation reaction of an aryl methyl ketone

[a] Institut für Chemie und Biochemie, Freie Universität Berlin, Takustraße 3, 14195 Berlin, Germany
E-mail: hans.reissig@chemie.fu-berlin.de
http://www.bcp.fu-berlin.de/en/chemie/chemie/forschung/OrgChem/reissig/index.html
[b] Institut für Physik, Humboldt Universität zu Berlin, Newtonstraße 15, 12489 Berlin, Germany
E-mail: rabe@physik.hu-berlin.de
http://www.physik.hu-berlin.de/pmm
Supporting information for this article is available on the WWW under http://dx.doi.org/10.1002/ejoc.201402178.

to form the central benzene ring by three subsequent aldol condensation steps.[9] In this report, we have exclusively followed pathway C and prepared the four desired star-shaped 1,3,5-tris[4-(4-pyridinyl)phenyl]benzene derivatives **1**–**4**, which consist of identical core units but are connected to differently substituted pyridine end groups (Scheme 2). We describe the synthesis of these compounds by straightforward transformations such as iron-catalyzed couplings of alkyl Grignard reagents,[10] halogenation reactions,[11] and the final acid-promoted cyclocondensation reaction of the corresponding methyl ketone derivatives.[12] The model compounds **1**–**4** showed remarkably different self-assembly at the graphite/phenyloctane solution interface as proven by STM investigations.

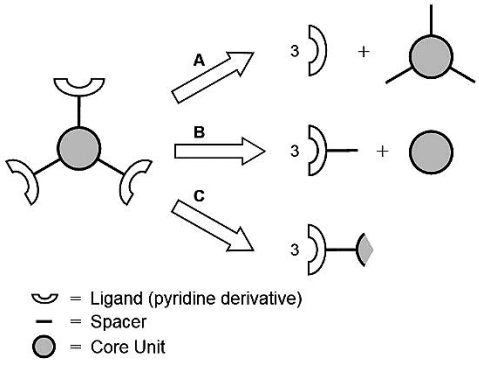

Scheme 1. Three strategies for the synthesis of star-shaped compounds with pyridine end groups.

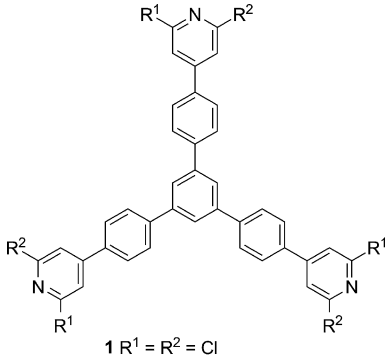

Scheme 2. Target compounds **1**–**4** required for STM studies.

Results and Discussion

The concept for the preparation of the 2,6-disubstituted pyridines was reported previously.[13] Starting from 2,6-dichloro-4-iodopyridine and (4-acetylphenyl)boronic acid, a Suzuki coupling with $Pd(PPh_3)_4$ as catalyst furnished aryl methyl ketone **5** in quantitative yield (Scheme 3). The cyclocondensation precursor **5** was then treated with silicon tetrachloride at 0 °C in ethanol[12a] to afford the first desired star-shaped compound **1** in 96% yield. Owing to the very poor solubility of **1**, it was not possible to obtain reasonable NMR spectra; however, the identity of **1** was clearly proven by mass spectrometry and by the STM investigations (see below).

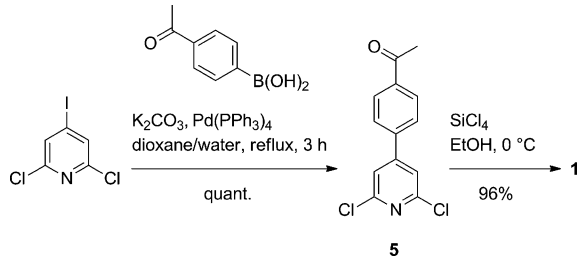

Scheme 3. Synthesis of D_{3h}-symmetrical star-shaped compound **1**.

From the hexachloro-substituted compound **1**, we attempted to perform an iron-catalyzed alkylation reaction[10] to obtain the corresponding hexaalkyl-substituted products **2** and **3** (Scheme 4), as was successfully applied in our previous published examples.[13] However, the poor solubility of these compounds or their preceding intermediates was problematic, and no full conversion was observed.

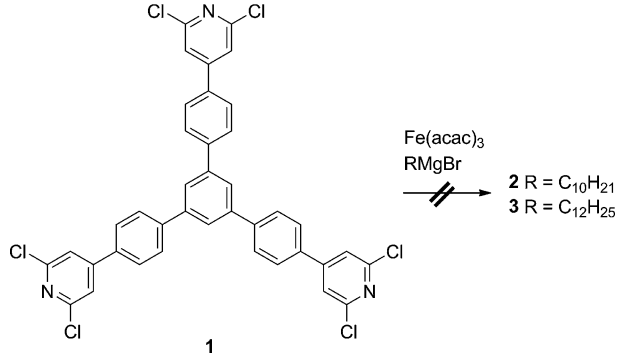

Scheme 4. Attempts to prepare alkyl-bearing D_{3h}-symmetrical star-shaped compounds **2** and **3** from precursor **1**.

The silicon tetrachloride mediated cyclocondensation of **14** and **15** to the desired star-shaped products **2** and **3** offers an alternative route (Scheme 5). Our synthesis started with the Suzuki coupling of 2,6-dichloro-4-iodopyridine and (4-formylphenyl)boronic acid to quantitatively yield aldehyde **6**, which was then treated with trimethyl orthoformate at 50 °C for 4 h to furnish the corresponding acetal **7** in 97% yield. Subsequently, the $Fe(acac)_3$-catalyzed (acac = acetylacetonate) reactions with decylmagnesium bromide or dodecylmagnesium bromide successfully afforded the two 2,6-dialkyl-substituted pyridine derivatives **8** and **9** in good yields. Deprotection by treatment with trifluoroacetic acid (TFA) resulted in the quantitative formation of aldehydes **10** and **11**, and the addition of methylmagnesium bromide afforded alcohols **12** and **13**. They were subsequently oxidized with Dess–Martin periodinane to give the cyclocondensation precursors **14** and **15** in good overall yields. In the final step, these aryl methyl ketones were again treated with silicon tetrachloride in ethanol to give the desired hexaalkyl-substituted star-shaped compounds **2** and **3** in moderate yields. Owing to solubility problems, it was not

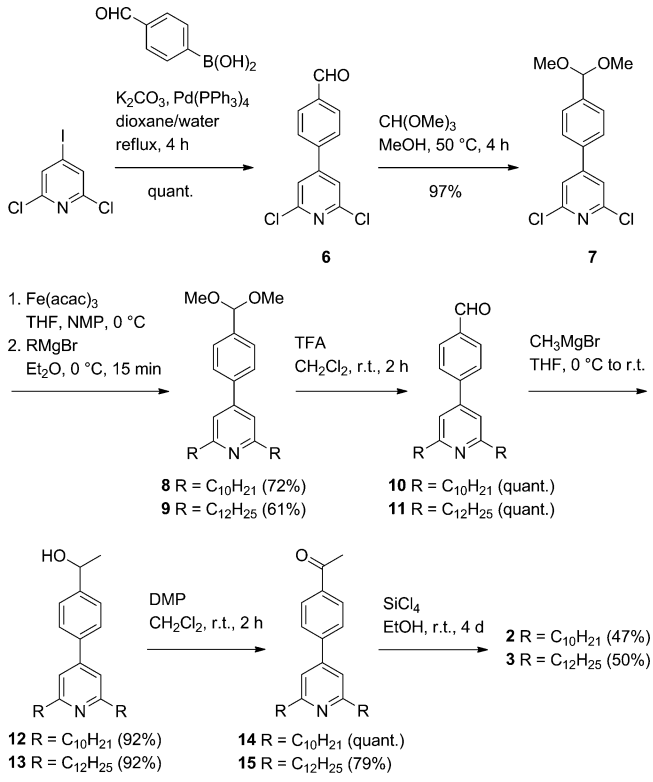

Scheme 5. Synthesis of alkyl-substituted D_{3h}-symmetrical star-shaped compounds **2** and **3**. DMP = Dess–Martin periodinane; NMP = *N*-methylpyrrolidone.

possible to record well-resolved NMR spectra. However, the ^{1}H NMR spectra clearly indicated that **2** and **3** were produced. In addition, the identity of the products was shown by mass spectrometry and by the STM studies (see below).

The synthesis of the C_{3h}-symmetrical star-shaped compound **4** was achieved by similar methods; however, a modification has to be realized to establish the lower symmetry. A chlorination reaction was implemented into the route to the unsymmetrical intermediate **18**, which is the key intermediate for the synthesis of C_{3h}-symmetrical star-shaped compounds (Scheme 6). The Suzuki coupling of 4-bromopyridine and (4-formylphenyl)boronic acid provided aldehyde **16** in quantitative yield. The treatment of **16** with trimethyl orthoformate gave acetal **17** in high yield. The subsequent chlorination was performed under the conditions described by Gros and Fort.[11] According to their method, the lithiation reaction selectively occurred at C-2 to afford the halogenated pyridine derivative **18** in moderate yield. A second Suzuki coupling with phenylboronic acid furnished the 2-phenyl-substituted derivative **19** in 87% yield. Under the conditions mentioned above, a second chlorination was performed to afford chlorinated compound **20** in 56% yield. The Fe(acac)$_3$-catalyzed reaction with decylmagnesium bromide provided the 2,6-disubstituted pyridine derivative **21** in good yield. Deprotection with TFA furnished aldehyde **22** almost quantitatively, and reaction with methyl Grignard reagent followed by oxidation of the resulting

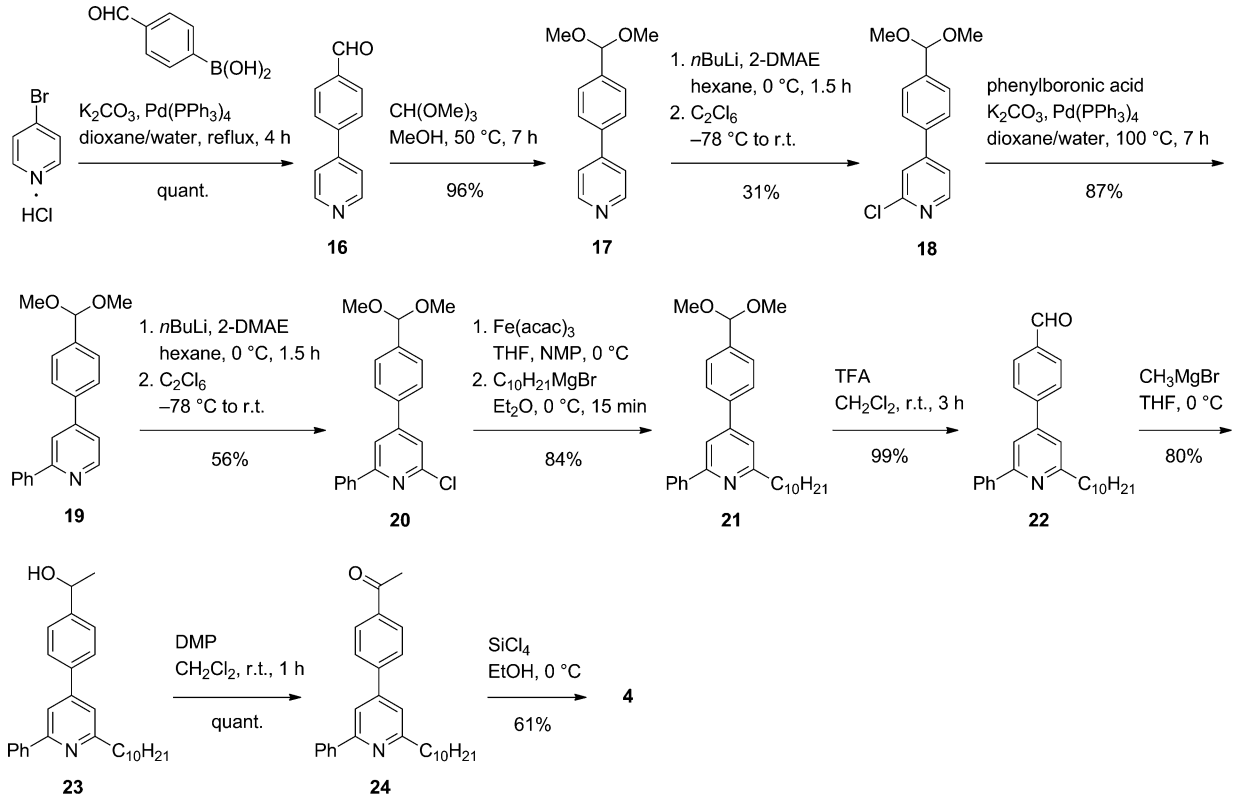

Scheme 6. Synthesis of C_{3h}-symmetrical star-shaped compound **4** with alkyl and phenyl substituents. 2-DMAE = 2-(dimethylamino)-ethanol; DMP = Dess–Martin periodinane; NMP = *N*-methylpyrrolidone.

alcohol afforded ketone **24** in high yield. The final acid-mediated cyclocondensation of **24** delivered the desired C_{3h}-symmetrical star-shaped target compound **4** in moderate yield (10 steps, 6% overall yield).

Molecular Self-Assembly at a Chemically Inert Solid–Liquid Interface

Scanning tunneling microscopy investigations were performed at the interface between a 1-phenyloctane solution and the basal plane of highly oriented pyrolytic graphite (HOPG; for further information, see the Experimental Section). The STM experiment with **1** indicates that this compound self-assembles in a structure with hexagonal symmetry and two molecules per unit cell (Figure 1). The central hole may be less regularly filled with solvent or molecules of **1**, which may partially protrude into the supernatant solution. In our proposed molecular model, the bright areas in the STM image, which correspond to high tunneling currents, provide the positions of the π systems, possibly including the phenyl rings of the solution.[14] On the one hand, the dark areas between the molecules designate the positions of the bulky chlorine atoms, which provide a relatively low tunneling current,[15] similarly to fluorine atoms.[14,16] On the other hand, the dark areas are due to interstices that seem to be caused by the electrostatic repulsion between the partially charged chlorine atoms. The counteracting force is provided by the thermodynamically quite generally favored adsorption of the large and rigid molecules from an organic solution at the interface with graphite.[17] In this model, each star interacts multivalently with three neighbors. The end groups of the stars interact such that three chlorine atoms surround one nitrogen atom; this indicates that this interaction is more favorable than the two chlorine atoms and the nitrogen atom between them facing the edge of a phenyl ring, for example. The bulky chloro substituents here cause the distance between the nitrogen atom and a hydrogen atom of the central core to be quite large, which leads to only a weak nitrogen–hydrogen dipole–dipole interaction. Hence, we observed a different pattern compared to those recently observed in investigations of D_{3h}-symmetrical compounds also without alkyl chains but bearing either only nitrogen[7a] or only iodine[7b] heteroatoms. In the first case, the packing was attributed to significant nitrogen–hydrogen dipole–dipole interactions, which are blocked in our case here by the chlorine atoms; in the second case iodine–iodine bonds were evoked, which we do not have here.

The self-assembly behavior of **2** and **3** was studied to compare the effect of different lengths of alkyl substituents. The obtained STM image of the decyl-substituted compound **2** and our proposed molecular model are shown in Figure 2. The D_{3h}-symmetrical star-shaped molecules pack in a 2D crystalline structure with hexagonal symmetry, which obviously differs from the observed hexagonal lattice of **1**. In contrast to **1**, the pyridyl moieties of **2** do not interdigitate, whereas its alkyl chains do owing to strong intermolecular van der Waals interactions. Therefore, it is not surprising that the alkyl chains play an important role in the self-assembly, as also shown in previous studies.[17] The bright areas in Figure 2 indicate the aromatic core and demonstrate the hexagonal arrangement of six molecules around a central gap. However, the detected (very low) tunneling current indicates the flexibility of the alkyl chains that point to the central hole.

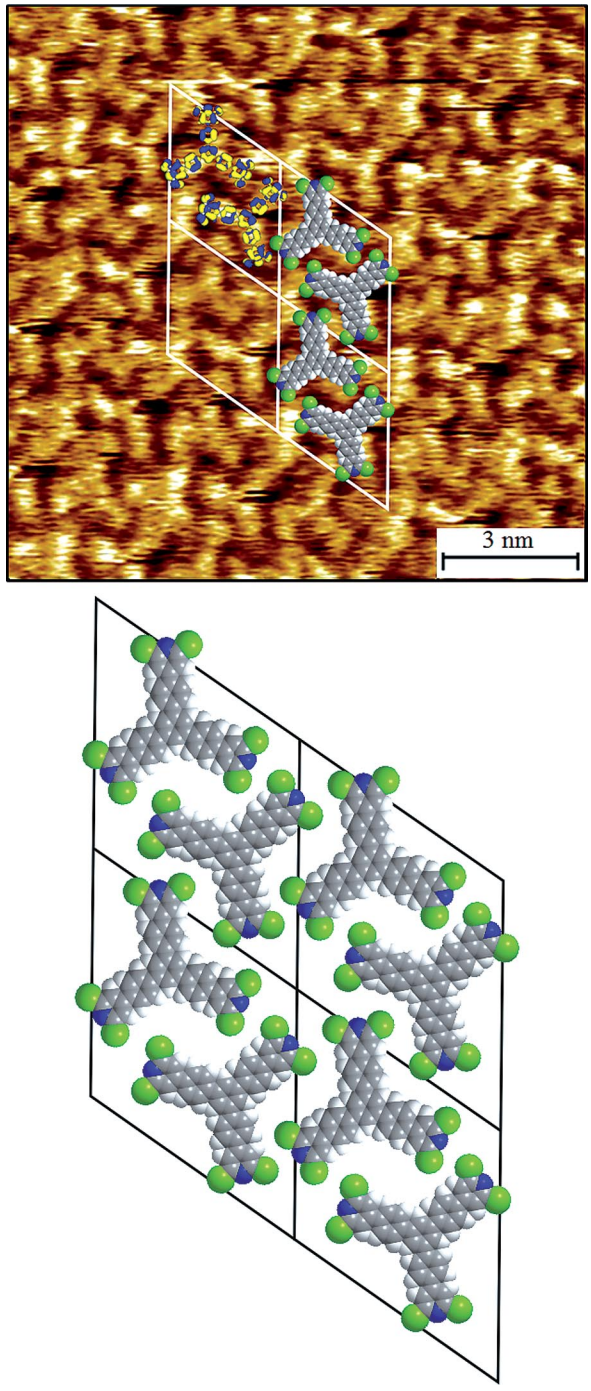

Figure 1. STM image of D_{3h}-symmetrical compound **1** showing a hexagonal arrangement and the proposed detailed molecular model (van der Waals and orbital models are plotted). Unit cell size: a = (2.98 ± 0.18) nm, b = (2.98 ± 0.18) nm, α = (63 ± 3)°, A = (7.30 ± 0.44) nm^2. U_s = –0.84 V, I_t = 21 pA.

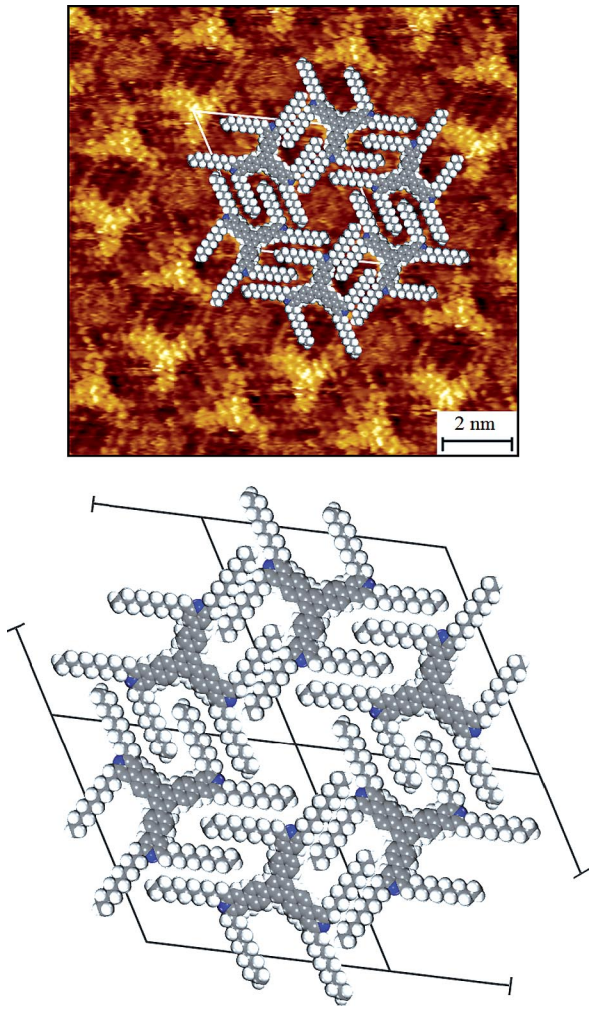

Figure 2. STM image of D_{3h}-symmetrical compound **2** showing a hexagonal arrangement as well as the proposed detailed molecular model (van der Waals models are plotted). Unit cell size: a = (4.00 ± 0.32) nm, b = (3.93 ± 0.31) nm, α = (63 ± 4)°, A = (14.0 ± 1.1) nm^2. U_s = –1.00 V, I_t = 30 pA.

The STM experiments with dodecyl-substituted compound **3** provided analogous results (Figure 3). The structural characteristics of the hexagonal arrangement of **3** are similar to those of **2**, but there are slight differences in the unit cell parameters. A lengthening of the alkyl chains from C_{10} in **2** to C_{12} in **3** leads as expected to a larger unit cell (14.0 vs. 18.4 nm^2). Interestingly, this modification had a significant effect on the detailed structural appearance, as the central hexagonal hole exhibits distinct tunneling probability. We tentatively propose that one more molecule is incorporated in the 2D structure owing to the larger central hole. However, the central hole covers an area of only 2.61 ± 0.18 nm^2, which means that the adsorption of the entire molecule is not possible. Hence, we assume that the alkyl chains protrude out of the 2D crystalline structure into the solution, similarly to the dimethyloctanyl side chains of hexa-*peri*-benzocoronenes, for example.[18] This is supported by the calculated molecular footprint of the aromatic core without alkyl chains (2.3 nm^2), which fits well with the determined area of the central hole in the STM image. Notably, this central molecule may exhibit a higher rotational mobility, which fits with the smeared-out contrast of the central hole. The symmetry of this pattern resembles the packing of bromo-substituted hexa-*peri*-benzocoronenes, which form D_{3h}-symmetric trimers that also pack hexagonally and leave a central hole that is filled with a monomer.[19]

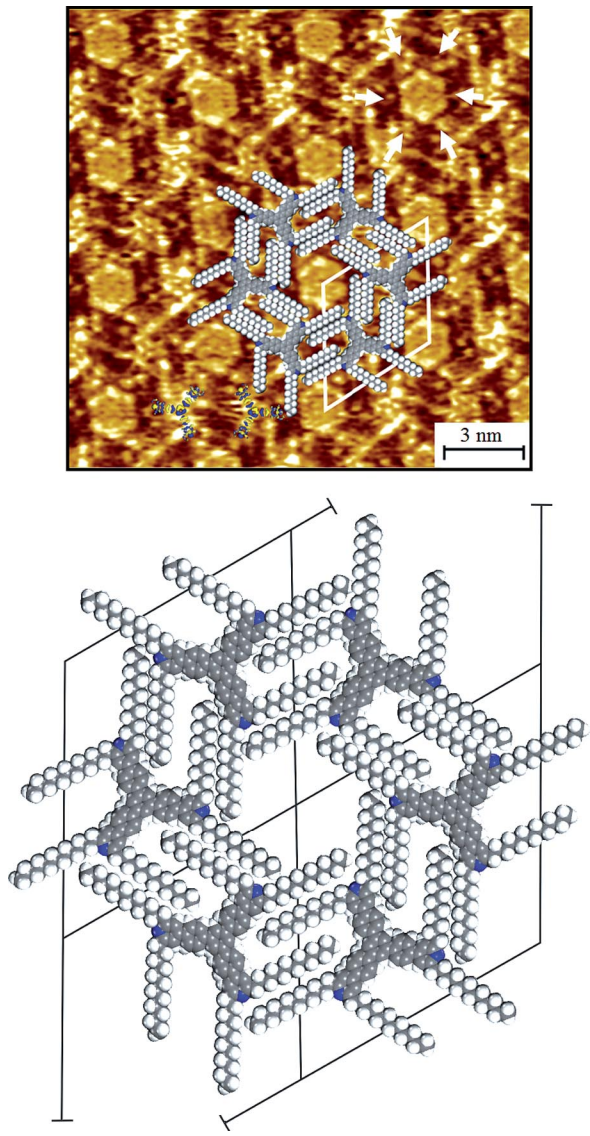

Figure 3. STM image of D_{3h}-symmetrical compound **3** showing a hexagonal arrangement as well as the proposed detailed molecular model (van der Waals and orbital models are plotted, the white arrows designate the pyridine end groups). Unit cell size: a = (4.63 ± 0.37) nm, b = (4.64 ± 0.37) nm, α = (59 ± 4)°, A = (18.4 ± 1.5) nm^2. U_s = –1.12 V, I_t = 32 pA.

The reduced symmetry of the C_{3h}-symmetrical pyridine derivative **4** leads to a remarkably different self-assembly behavior. This compound self-assembles in long chains with two oppositely oriented molecules per unit cell and with chains (lamellae) packed parallel to each other (Figure 4).

There are two types of interdigitation in the proposed molecular model. On the one hand, the phenyl moieties interact strongly to produce an interdigitated aromatic scaffold along the lamellae, and on the other hand, the alkyl chains interact through substantial van der Waals interactions. Apparently, both the alkyl chains and the phenyl group play an important role in the formation of the specific lamellar structure. The latter cause the dark areas parallel to the lamellae in the STM image. Nagata and Ogawa reported a similar behavior of C_2-symmetrical *N*,*N*′-dialkylnaphthalenediimide derivatives, for which the formed lattices change as a function of the alkyl chain length.[20] In our system, the alkyl chain lengths do not dominate the self-assembly as hexagonal structures were determined in the STM experiments of **2** and **3**. This is the first example that shows that the self-assembly of star-shaped molecules can be dramatically changed by reducing their symmetry from D_{3h} to C_{3h} by using two different moieties (aryl and alkyl) at the pyridine ligand.

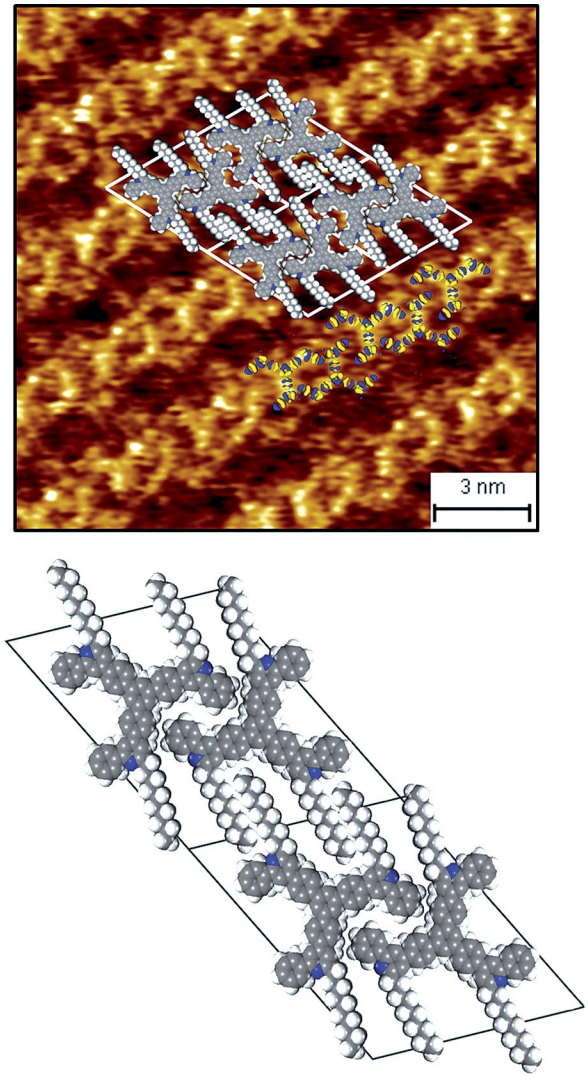

Figure 4. STM image of C_{3h}-symmetrical compound **4** showing a lamellar arrangement as well as the proposed detailed molecular model (van der Waals and orbital models are plotted). Unit cell size: a = (3.04 ± 0.24) nm, b = (3.86 ± 0.30) nm, α = (65 ± 3)°, A = (10.9 ± 0.87) nm^2. U_s = –1.07 V, I_t = 43 pA.

Conclusions

We have successfully applied our previously reported methodology to the synthesis of new star-shaped compounds with 2,6-disubstituted pyridine units as end groups. The applied methods are straightforward and flexible and should be applicable to other compounds of this type. The efficient generation of the central benzene ring by the acid-mediated cyclocondensation of aryl methyl ketone precursors should also allow the preparation of other D_{3h}- and C_{3h}-symmetrical systems. To realize the lower symmetry, we implemented a monochlorination step in our route. The synthesized star-shaped compounds were investigated by STM measurements and showed remarkably different self-assembled monolayers at HOPG. We demonstrated that a reduction of symmetry from D_{3h} to C_{3h} leads to entirely different behavior. The D_{3h}-symmetrical compounds **1**–**3** pack in 2D crystalline structures with hexagonal symmetry, whereas the C_{3h}-symmetrical derivative **4** forms long chains that are packed parallel to each other. Our systematic study of substituents effects on self-assembly processes will help us to understand and predict these phenomena. In addition, C_3-symmetrical compounds with pyridine end groups such as **1**–**4** are interesting owing to their ability to form complexes with metal ions on surfaces for investigation of their influence on aggregation and the effect of multivalency.[21] Preliminary investigations of the properties of these derivatives are encouraging, and the complex formation is currently under investigation.

Experimental Section

Scanning Tunneling Microscopy: STM experiments were performed at room temperature at the interface between a freshly cleaved highly oriented pyrolytic graphite (HOPG) surface and an almost saturated solution of the sample in 1-phenyloctane (Aldrich) by employing a home-made set-up at a scan speed between 10 and 50 lines/s. The STM images were recorded in constant-current mode (STM height images). After visualization of the HOPG lattice, a drop of the prepared solution was applied to the basal plane of HOPG. The STM images were corrected with respect to the hexagonal HOPG lattice underneath by exploiting the SPIP software. In this way, the unit cell of the adsorbate crystal could be defined with a high degree of precision. The implemented space-filling models are based on standard van der Waals parameters. The molecular orbitals were calculated with the DMol3 interface of Accelrys Materials Studio by using the local-density approximation method and Perdew–Wang correlation.[22]

General Methods for the Syntheses: See Supporting Information. The multiplicity of complex AA′XX′ systems is abbreviated with d*, and only the largest coupling constant is given.

Typical Procedure A for Suzuki Coupling Reactions: To a degassed solution of halogenated pyridine, K_2CO_3 (3 equiv.), and boronic acid (1.5 equiv.) in dioxane (10 mL/mmol) and water (2.5 mL/mmol) was added $Pd(PPh_3)_4$ (5 mol-%). The resulting mixture was

heated to reflux until complete conversion (TLC control). After cooling to room temperature and the addition of water, the mixture was extracted with CH_2Cl_2. The combined organic layers were dried with $MgSO_4$, filtered, and concentrated, and the residue was purified by silica gel chromatography (hexanes/ethyl acetate) to give the desired Suzuki coupling product.

Typical Procedure B for Cyclocondensation Reactions: To a stirred solution of aryl methyl ketone derivative in dry EtOH (1 mL/10 mmol) was added $SiCl_4$ (10 equiv.) at 0 °C. The resulting mixture was stirred at room temperature overnight and quenched by the slow addition of water. Filtration of the resulting precipitate afforded the expected star-shaped derivative.

Typical Procedure C for Coupling Reactions with Grignard Reagents. Grignard Formation: To a stirred suspension of magnesium turnings (10 equiv.) and an iodine crystal in dry Et_2O (1 mL/mmol) was added the corresponding bromoalkane (2.5 equiv.). To initiate the reaction, it is sometimes necessary to heat the mixture. The reaction mixture was heated to reflux for 1 h and then cooled to room temperature. **Coupling Reaction:** The solution of the Grignard reagent was added in one portion to a solution of $Fe(acac)_3$ (10 mol-%) and the corresponding chloropyridine derivative in dry tetrahydrofuran (THF; 10 mL/mmol) and *N*-methylpyrrolidone (1 mL/mmol) at 0 °C. The mixture was stirred for 15 min, quenched by the addition of brine, and extracted with CH_2Cl_2. The combined organic layers were dried with $MgSO_4$ and concentrated to dryness. The residue was purified by silica gel column chromatography (hexanes/ethyl acetate) to give the desired compound.

4-(2,6-Dichloropyridin-4-yl)benzaldehyde (6): According to general procedure A, 2,6-dichloro-4-iodopyridine (830 mg, 3.03 mmol), (4-formylphenyl)boronic acid (459 mg, 3.06 mmol), K_2CO_3 (1.67 g, 12.1 mmol), and $Pd(PPh_3)_4$ (175 mg, 0.15 mmol) in dioxane (24 mL) and water (8 mL) were heated to reflux for 4 h. After workup, the crude solid was washed with hexanes to provide the expected product **6** as a colorless solid (764 mg, quant.). M.p. 160–164 °C. ^{1}H NMR (400 MHz, $CDCl_3$): δ = 7.51 (s, 2 H, Py-H), 7.76 (d*, J = 8.4 Hz, 2 H, Ar-H), 8.02 (d*, J = 8.4 Hz, 2 H, Ar-H), 10.10 (s, 1 H, CHO) ppm. ^{13}C NMR (126 MHz, $CDCl_3$): δ = 121.0, 127.9, 130.5 (3 d, Py, 2 Ar-H), 137.2, 141.3, 151.4, 152.4 (4 s, 2 Ar, C-2, C-4), 191.3 (d, CHO) ppm. IR (KBr): $\tilde{\nu}$ = 3110–2745 (=C–H, C–H), 1710 (C=O), 1610–1360 (C=C, C=N) cm^{-1}.

2,6-Dichloro-4-[4-(dimethoxymethyl)phenyl]pyridine (7): A solution of aldehyde **6** (200 mg, 0.79 mmol), trimethyl orthoformate (0.50 mL, 3.97 mmol), and *p*-toluenesulfonic acid (8 mg, 46 μmol) in MeOH (10 mL) was stirred at 50 °C for 4 h. The reaction mixture was diluted with Et_2O and washed with 1 M aq. $NaHCO_3$ solution. The combined organic layers were dried with $MgSO_4$, filtered, and concentrated to afford acetal **7** (230 mg, 97%) as a grey solid. M.p. 77–79 °C. ^{1}H NMR (500 MHz, $CDCl_3$): δ = 3.29 (s, 6 H, OCH_3), 5.41 (s, 1 H, OCHO), 7.42 (s, 2 H, Py-H), 7.55 (br. s, 4 H, Ar-H) ppm. ^{13}C NMR (126 MHz, $CDCl_3$): δ = 52.7 (q, OCH_3), 102.4, 120.7, 127.0, 127.8 (4 d, OCHO, Py-H, 2 Ar-H), 135.7, 140.4, 151.1, 153.5 (4 s, 2 Ar, C-2, C-4) ppm. IR (KBr): $\tilde{\nu}$ = 3075–2885 (=C–H, C–H), 2830 (O–CH_3), 1580–1360 (C=C, C=N) cm^{-1}. HRMS (ESI-TOF): calcd. for $C_{14}H_{14}Cl_2NO_2$ $[M + H]^+$ 298.0396; found 298.0323. $C_{14}H_{13}Cl_2NO_2$ (298.2): calcd. C 56.39, H 4.39, N 4.70; found C 56.24, H 4.54, N 4.29.

4-[4-(Dimethoxymethyl)phenyl]-2,6-didodecylpyridine (9): According to general procedure C, Mg (326 mg, 13.4 mmol), 1-bromododecane (0.80 mL, 3.35 mmol) in Et_2O (5 mL), $Fe(acac)_3$ (47 mg, 0.1 mmol), and dichloropyridine derivative **7** (200 mg, 0.67 mmol) in THF (10 mL) and *N*-methylpyrrolidone (1 mL) gave **9** (233 mg, 61%) as a yellow oil after purification on silica gel (hexanes to hexanes/ethyl acetate 95:5). ^{1}H NMR (500 MHz, $CDCl_3$): δ = 0.87 (t, J = 6.9 Hz, 6 H, 2 CH_3), 1.20–1.40 (m, 36 H, 18 CH_2), 1.69–1.77 (m, 4 H, 2 CH_2), 2.80 (m_c, 4 H, 2 CH_2), 3.36 (s, 6 H, OCH_3), 5.45 (s, 1 H, OCHO), 7.17 (s, 2 H, Py-H), 7.54 (d*, J = 8.2 Hz, 2 H, Ar-H), 7.63 (d*, J = 8.2 Hz, 2 H, Ar-H) ppm. ^{13}C NMR (126 MHz, $CDCl_3$): δ = 14.1 (q, CH_3), 22.7, 29.3, 29.50, 29.54, 29.58, 29.63, 29.64, 29.66, 30.3, 31.9, 38.7 (11 t, CH_2), 52.7 (q, OCH_3), 102.7, 117.8, 126.9, 127.3 (4 d, OCHO, Py-H, Ar-H), 138.5, 139.1, 148.9, 162.5 (4 s, 2 Ar, C-4, C-2) ppm. IR (ATR): $\tilde{\nu}$ = 2990–2845 (=C–H, C–H), 1600–1350 (C=C, C=N) cm^{-1}. HRMS (ESI-TOF): calcd. for $C_{38}H_{64}NO_2$ $[M + H]^+$ 566.4932; found 566.4922.

4-(2,6-Didodecylpyridin-4-yl)benzaldehyde (11): TFA (2.0 mL, 26 mmol) was added dropwise to a solution of acetal **9** (230 mg, 0.41 mmol) in CH_2Cl_2 (5 mL). The mixture was stirred at room temperature for 2 h and quenched with saturated aqueous $NaHCO_3$ solution. The organic phase was washed with saturated aqueous $NaHCO_3$ solution until pH = 7 was reached. The organic layer was dried with $MgSO_4$, filtered, and concentrated to give aldehyde **11** (220 mg, quant.) as a yellow oil. ^{1}H NMR (500 MHz, $CDCl_3$): δ = 0.87 (t, J = 7.0 Hz, 6 H, 2 CH_3), 1.20–1.40 (m, 36 H, 18 CH_2), 1.75 (quint, J = 7.7 Hz, 4 H, 2 CH_2), 2.84 (m_c, 4 H, 2 CH_2), 7.19 (s, 2 H, Py-H), 7.78 (d*, J = 8.2 Hz, 2 H, Ar-H), 7.98 (d*, J = 8.2 Hz, 2 H, Ar-H), 10.08 (s, 1 H, CHO) ppm. ^{13}C NMR (126 MHz, $CDCl_3$): δ = 14.1 (q, CH_3), 22.7, 29.3, 29.49, 29.53, 29.58, 29.65, 29.65, 29.67, 30.2, 31.9, 38.7 (11 t, CH_2), 117.9, 127.8, 130.3 (3 d, Py-H, Ar-H), 136.2, 162.8 (2 s, C-4, C-2), 191.7 (d, CHO) ppm. IR (ATR): $\tilde{\nu}$ = 2955–2845 (=C–H, C–H), 1690 (C=O), 1595–1425 (C=C, C=N) cm^{-1}. HRMS (ESI-TOF): calcd. for $C_{36}H_{58}NO$ $[M + H]^+$ 520.4513; found 520.4507.

1-[4-(2,6-Didodecylpyridin-4-yl)phenyl]ethanol (13): A solution of methylmagnesium bromide (0.50 mL, 1.54 mmol, 3 M in THF) was added dropwise at 0 °C to a solution of aldehyde **11** (200 mg, 0.38 mmol) in dry THF (8 mL). The mixture was stirred at room temperature for 1 h and then quenched with water. The THF was removed under reduced pressure, and the residue was diluted with CH_2Cl_2 and washed with water. The combined organic layers were dried with $MgSO_4$ and concentrated to dryness to give alcohol **13** (190 mg, 92%) as a yellow oil. ^{1}H NMR (500 MHz, $CDCl_3$): δ = 0.87 (t, J = 7.0 Hz, 6 H, 2 CH_3), 1.20–1.40 (m, 36 H, 18 CH_2), 1.53 (d, J = 6.5 Hz, 3 H, CH_3), 1.69–1.76 (m, 4 H, 2 CH_2), 2.79 (m_c, 4 H, 2 CH_2), 4.97 (q, J = 6.5 Hz, 1 H, CHOH), 7.15 (s, 2 H, Py-H), 7.47 (d*, J = 8.2 Hz, 2 H, Ar-H), 7.60 (d*, J = 8.2 Hz, 2 H, Ar-H) ppm. ^{13}C NMR (126 MHz, $CDCl_3$): δ = 14.1 (q, CH_3), 22.7 (t, CH_2), 25.3 (q, CH_3), 29.3, 29.49, 29.53, 29.57, 29.62, 29.65, 30.3, 31.9, 31.9, 38.6 (10 t, CH_2), 69.9 (d, CHOH), 117.7, 125.9, 127.1 (3 d, Py-H, Ar-H), 138.1, 146.5, 148.5, 162.4 (4 s, 2 Ar, C-4, C-2) ppm. IR (ATR): $\tilde{\nu}$ = 3295 (OH), 2960–2850 (=C–H, C–H), 1600–1365 (C=C, C=N) cm^{-1}. HRMS (ESI-TOF): calcd. for $C_{37}H_{62}NO$ $[M + H]^+$ 536.4826; found 536.4838.

1-[4-(2,6-Didodecylpyridin-4-yl)phenyl]ethanone (15): To a solution of alcohol **13** (180 mg, 0.34 mmol) in dry CH_2Cl_2 (10 mL) was added Dess–Martin periodinane (200 mg, 0.47 mmol), and the mixture was stirred at room temperature for 2 h. $Na_2S_2O_3$ (266 mg, 1.68 mmol) and Et_2O (5 mL) were added, and the mixture was stirred for 1 h. After the addition of water, the mixture was extracted with CH_2Cl_2. The combined organic layers were dried with $MgSO_4$, filtered, and concentrated, and the residue was purified by silica gel chromatography (hexanes/ethyl acetate, 95:5) to give ketone **15** (141 mg, 79%) as a colorless solid. M.p. 52–53 °C. ^{1}H NMR (500 MHz, $CDCl_3$): δ = 0.87 (t, J = 7.0 Hz, 6 H, 2 CH_3), 1.20–1.40 (m, 36 H, 18 CH_2), 1.74 (m_c, 4 H, 2 CH_2), 2.65 (s, 3 H, CH_3), 2.82 (m_c, 4 H, 2 CH_2), 7.18 (s, 2 H, Py-H), 7.71 (d*, J =

8.5 Hz, 2 H, Ar-H), 8.05 (d*, J = 8.5 Hz, 2 H, Ar-H) ppm. ^{13}C NMR (126 MHz, $CDCl_3$): δ = 14.1 (q, CH_3), 22.7 (t, CH_2), 26.7 (q, CH_3), 29.3, 29.46, 29.48, 29.55, 29.61, 29.62, 29.64, 30.3, 31.9, 38.7 (10 t, CH_2), 117.8, 127.3, 128.9 (3 d, Py-H, 2 Ar-H), 136.9, 143.6, 147.5, 162.8, (4 s, 2 Ar, C-4, C-2), 197.6 (s, CO) ppm. IR (KBr): $\tilde{\nu}$ = 2960–2850 (=C–H, C–H), 1680 (C=O), 1600–1270 (C=C, C=N) cm^{-1}. HRMS (ESI-TOF): calcd. for $C_{37}H_{60}NO$ $[M + H]^+$ 534.4669; found 534.4687. $C_{37}H_{59}NO$ (533.9): calcd. C 83.24, H 11.14, N 2.62; found C 82.95, H 11.29, N 2.55.

1,3,5-Tris[(2,6-didodecylpyridin-4-yl)phenyl]benzene (3): According to general procedure B: To a stirred solution of ketone **15** (100 mg, 0.19 mmol) in dry EtOH (1 mL) was added $SiCl_4$ (0.26 mL, 2.25 mmol) at 0 °C. The mixture was warmed overnight to room temperature and stirred for another 4 d. After the addition of water, the aqueous phase was extracted with CH_2Cl_2 to afford the crude product (151 mg). A portion of the crude product (100 mg) was recrystallized from pyridine/hexanes to afford **3** (32 mg, calcd. yield 50%) as a yellow solid. Owing to the very low solubility of **3**, only a moderately resolved ^1H NMR spectrum could be recorded. ^1H NMR (700 MHz, $CDCl_3$): δ = 0.89 (t, J = 6.9 Hz, 18 H, 6 CH_3), 1.23–1.45 (m, 84 H, 42 CH_2), 1.94 (br. s, 12 H, 6 CH_2), 3.42 (br. s, 12 H, 6 CH_2), 7.29 (s, 6 H, Py-H), 7.64 (br. s, 6 H, Ar-H), 7.89 (br. s, 6 H, Ar-H), 7.95 (br. s, 6 H, Py) ppm. IR (ATR): $\tilde{\nu}$ = 2955–2850 (C–H), 1625 (C=C, C=N) cm^{-1}. HRMS (ESI-TOF): calcd. for $C_{111}H_{172}N_3$ $[M + H]^+$ 1547.3546, $[M + 2 H]^{2+}$ 774.1810, $[M + 3 H]^{3+}$ 516.4564; found 1547.3603, 774.1860, 516.4620.

Supporting Information (see footnote on the first page of this article): Experimental procedures, analytical data and copies of the NMR spectra.

Acknowledgments

The generous support by the Deutsche Forschungsgemeinschaft (SFB 765), the Evonik Foundation (PhD fellowship for D. T.), and Bayer HealthCare is gratefully acknowledged. We thank Susie Gröper for preliminary STM studies and Dr. Reinhold Zimmer for help during the preparation of this manuscript.

[1] a) D. J. Kushner, *Bacteriol. Rev.* **1969**, *33*, 302–345; b) A. C. Mendes, E. T. Baran, R. L. Reis, H. S. Azevedo, *Wiley Interdiscip. Rev. Nanomed. Nanobiotechnol.* **2013**, *5*, 582–612; c) D. Philp, J. F. Stoddart, *Angew. Chem. Int. Ed. Engl.* **1996**, *35*, 1154–1196; *Angew. Chem.* **1996**, *108*, 1242–1286.

[2] a) G. Maruccio, R. Cingolani, R. Rinaldi, *J. Mater. Chem.* **2004**, *14*, 542–554; b) S. A. DiBenedetto, A. Facchetti, M. A. Ratner, T. J. Marks, *Adv. Mater.* **2009**, *21*, 1407–1433; c) R. L. Carroll, C. B. Gorman, *Angew. Chem. Int. Ed.* **2002**, *41*, 4378–4400; *Angew. Chem.* **2002**, *114*, 4556–4579.

[3] C. P. Collier, G. Mattersteig, E. W. Wong, Y. Luo, K. Beverly, J. Sampaio, F. M. Raymo, J. F. Stoddart, J. R. Heath, *Science* **2000**, *289*, 1172–1175.

[4] a) S. J. H. Griessl, M. Lackinger, F. Jamitzky, T. Markert, M. Hietschold, W. M. Heckl, *Langmuir* **2004**, *20*, 9403–9407; b) L. Kampschulte, M. Lackinger, A.-K. Maier, R. S. K. Kishore, S. Griessl, M. Schmittel, W. M. Heckl, *J. Phys. Chem. B* **2006**, *110*, 10829–10836; c) K. Eichhorst-Gerner, A. Stabel, G. Moessner, D. Declerq, S. Valiyaveettil, V. Enkelmann, K. Müllen, J. P. Rabe, *Angew. Chem. Int. Ed. Engl.* **1996**, *35*, 1492–1495; *Angew. Chem.* **1996**, *108*, 1599–1602.

[5] C.-A. Palma, M. Cecchini, P. Samorì, *Chem. Soc. Rev.* **2012**, *41*, 3713–3730.

[6] T. Lechel, M. Gerhard, D. Trawny, B. Brusilowskij, L. Schefzig, R. Zimmer, J. P. Rabe, D. Lentz, C. A. Schalley, H.-U. Reissig, *Chem. Eur. J.* **2011**, *17*, 7480–7491.

[7] a) A. Ciesielski, P. J. Szabelski, W. Rżysko, A. Cadeddu, T. R. Cook, P. J. Stang, P. Samorì, *J. Am. Chem. Soc.* **2013**, *135*, 6942–6950; b) F. Silly, *J. Phys. Chem. C* **2013**, *117*, 20244–20249.

[8] a) H. L. Anderson, C. J. Walter, A. Vidal-Ferran, R. A. Hay, P. A. Lowden, J. K. M. Sanders, *J. Chem. Soc. Perkin Trans. 1* **1995**, 2275–2279; b) N. Kobayashi, M. Kijima, *J. Mater. Chem.* **2008**, *18*, 1037–1045; c) S. Winter, E. Weber, L. Eriksson, I. Csoregh, *New J. Chem.* **2006**, *30*, 1808–1819.

[9] C. Engler, H. E. Berthold, *Ber. Dtsch. Chem. Ges.* **1874**, *7*, 1123–1125.

[10] A. Fürstner, A. Leitner, M. Méndez, H. Krause, *J. Am. Chem. Soc.* **2002**, *124*, 13856–13863.

[11] P. Gros, S. Choppin, J. Mathieu, Y. Fort, *J. Org. Chem.* **2001**, *67*, 234–237.

[12] a) S. S. Elmorsy, A. Pelter, K. Smith, *Tetrahedron Lett.* **1991**, *32*, 4175–4176; b) B. P. Dash, R. Satapathy, J. A. Maguire, N. S. Hosmane, *Org. Lett.* **2008**, *10*, 2247–2250; c) Y.-J. Li, H. Sasabe, S.-J. Su, D. Tanaka, T. Takeda, Y.-J. Pu, J. Kido, *Chem. Lett.* **2010**, *39*, 140–141.

[13] L. Vandromme, H.-U. Reissig, S. Gröper, J. P. Rabe, *Eur. J. Org. Chem.* **2008**, 2049–2055.

[14] R. Lazzaroni, A. Calderone, J. L. Brédas, J. P. Rabe, *J. Chem. Phys.* **1997**, *107*, 99–105.

[15] C. L. Claypool, F. Faglioni, W. A. Goddard III, H. B. Gray, N. S. Lewis, R. A. Marcus, *J. Phys. Chem. B* **1997**, *101*, 5978–5995.

[16] A. Stabel, L. Dasaradhi, D. O'Hagan, J. P. Rabe, *Langmuir* **1995**, *11*, 1427–1430.

[17] P. Samorì, N. Severin, K. Müllen, J. P. Rabe, *Adv. Mater.* **2000**, *12*, 579–582.

[18] P. Samorì, A. Fechtenkötter, F. Jäckel, T. Böhme, K. Müllen, J. P. Rabe, *J. Am. Chem. Soc.* **2001**, *123*, 11462–11467.

[19] S. Ito, M. Wehmeier, J. D. Brand, C. Kübel, R. Epsch, J. P. Rabe, K. Müllen, *Chem. Eur. J.* **2000**, *6*, 4327–4342.

[20] Y. Miyake, T. Nagata, H. Tanaka, M. Yamazaki, M. Ohta, R. Kokawa, T. Ogawa, *ACS Nano* **2012**, *6*, 3876–3887.

[21] Review: C. Fasting, C. A. Schalley, M. Weber, O. Seitz, S. Hecht, B. Koksch, J. Dernedde, C. Graf, E.-W. Knapp, R. Haag, *Angew. Chem. Int. Ed.* **2012**, *51*, 10472–10498; *Angew. Chem.* **2012**, *124*, 10622–10650.

[22] J. P. Perdew, Y. Wang, *Phys. Rev. B* **1992**, *45*, 13244–13249.

Received: March 3, 2014
Published Online: June 30, 2014

